



Contents lists available at ScienceDirect

## Sensors and Actuators A: Physical

journal homepage: [www.elsevier.com/locate/sna](http://www.elsevier.com/locate/sna)



# Surface patterned polymer micro-cantilever arrays for sensing

Prabitha Urwyler<sup>a,b,\*</sup>, Helmut Schiff<sup>a</sup>, Jens Gobrecht<sup>a</sup>, Oskar Häfeli<sup>c</sup>,  
Mirco Altana<sup>d</sup>, Felice Battiston<sup>e</sup>, Bert Müller<sup>b</sup>

<sup>a</sup> Paul Scherrer Institut, Laboratory for Micro- and Nanotechnology, 5232 Villigen PSI, Switzerland

<sup>b</sup> University of Basel, Biomaterials Science Center, c/o University Hospital, 4031 Basel, Switzerland

<sup>c</sup> University of Applied Sciences Northwestern Switzerland, Institute of Polymer Engineering, 5210 Windisch, Switzerland

<sup>d</sup> University of Applied Sciences Northwestern Switzerland, Institute of Polymer Nanotechnology, 5210 Windisch, Switzerland

<sup>e</sup> Concentris GmbH, Davidsbodenstrasse 63, 4012 Basel, Switzerland

### ARTICLE INFO

#### Article history:

Received 29 September 2010

Received in revised form 7 December 2010

Accepted 9 December 2010

Available online xxx

#### PACS:

81.16.Nd (nanolithography)

81.20.Hy (molding)

87.19.It (sensory systems)

87.80.Ek (micromechanical techniques)

87.85.Rs (nanotechnology-applications)

87.85.dh (cells on a chip)

#### Keywords:

Micro-cantilever

Polymer

Sensor

Injection molding

Nanoimprint lithography

Stamps

Mold

### ABSTRACT

Microinjection molding was employed to fabricate low-cost polymer cantilever arrays for sensor applications. Cantilevers with micrometer dimensions and aspect ratios as large as 10 were successfully manufactured from polymers, including polypropylene and polyvinylidene fluoride. The cantilevers perform similar to the established silicon cantilevers, with *Q*-factors in the range of 10–20. Static deflection of gold coated polymer cantilevers was characterized with heat cycling and self-assembled monolayer formation of mercaptohexanols. A hybrid mold concept allows easy modification of the surface topography, enabling customized mechanical properties of individual cantilevers. Combined with functionalization and surface patterning, the cantilever arrays are qualified for biomedical applications.

© 2011 Elsevier B.V. All rights reserved.

## 1. Introduction

Micro-cantilevers ( $\mu$ Cs), similar to those used in scanning force microscopes (SFM), have become increasingly popular as transducers in chemical and biological sensors [1–8]. They convert physical, chemical, and biological stimuli into measurable signals. Various detection methods have been introduced to measure the bending of the  $\mu$ Cs in the range of few nanometers with extremely high accuracy. A compelling feature of  $\mu$ C sensors is that they operate in air, vacuum, or liquid environment [7]. Like many micro-machined

devices,  $\mu$ Cs are typically made from glass, silicon or other rigid materials. In the field of biomedicine, silicon-based  $\mu$ Cs have to be cleaned or even sterilized for repetitive use. For single usage they are often too expensive. The fabrication is based upon single crystalline silicon wafers to be processed in cleanroom facilities. The high costs compromise many applications and calls for low-cost, disposable sensing elements. Polymer materials offer tailored physical and chemical properties to be combined with low-cost mass production. Therefore, compared to silicon-based  $\mu$ Cs the polymeric  $\mu$ Cs can exhibit better biocompatibility and much better adaptability of rapid prototyping along with mechanical properties, which make them particularly sensitive [7]. Despite these advantages polymeric  $\mu$ C arrays are not yet commercially available. Polymer  $\mu$ Cs can be prepared in a variety of ways, whereas the type of polymer often determines the fabrication method [7,9]. So far, polymer  $\mu$ Cs were realized using photolithography. It is limited to the suitable materials and the  $\mu$ Cs fabrication is rather expensive [10]. Molding of microcomponents from thermoplastic

\* Corresponding author at: Paul Scherrer Institut, Laboratory for Micro- and Nanotechnology, ODRA 117, 5232 Villigen PSI, Switzerland. Tel.: +41 56 3102430.

E-mail addresses: [prabitha.urwyler@psi.ch](mailto:prabitha.urwyler@psi.ch) (P. Urwyler), [helmut.schiff@psi.ch](mailto:helmut.schiff@psi.ch) (H. Schiff), [jens.gobrecht@psi.ch](mailto:jens.gobrecht@psi.ch) (J. Gobrecht), [oskar.haefeli@fhnw.ch](mailto:oskar.haefeli@fhnw.ch) (O. Häfeli), [mirco.altana@fhnw.ch](mailto:mirco.altana@fhnw.ch) (M. Altana), [battiston@concentris.ch](mailto:battiston@concentris.ch) (F. Battiston), [bert.mueller@unibas.ch](mailto:bert.mueller@unibas.ch) (B. Müller).

polymers has become a routinely used industrial production process and is one of the most promising fabrication techniques for non-electronic micro devices [11]. Fabrication costs of molded parts are hardly affected by the complexity of the design. Once a mold insert is available, several thousand parts can be molded with modest effort. Furthermore, different polymers can be used to obtain parts of almost identical shape with a high degree of reproducibility. Micro-patterns on the mold can be replicated into the molded device, too, making it possible to integrate different dimensions and topographies into one single tool. The mechanical properties of polymer  $\mu$ Cs can be tailored choosing appropriate dimensions and surface morphologies. The cost of the raw material in most cases is negligibly low, because only small quantities are required for micrometer-sized components. Therefore, parts fabricated by micromolding, even from high-end materials, are suitable for applications requiring low-cost and disposable components. Several thermoplastic molding processes such as hot embossing, injection molding (IM), injection compression molding and thermoforming give rise to micro-parts with high precision and repeatability [11,12]. Polymeric replication techniques based on nanoimprint and casting of curable polymers can be used to produce structures with sub-100 nm resolutions [13,14]. The hot embossing and the IM seem to be the most industrially viable processes for molded micro-parts [15]. Polystyrene (PS) cantilever beams of thicknesses between 2 and 40  $\mu$ m with a stiffness ranging from 0.01 to 10 N m<sup>-1</sup> have been produced using IM [10]. The acceptance of  $\mu$ C sensors in research and commercial, analytic applications crucially depends on the robustness, the ease of use, the reproducibility and finally the price. The question arises if disposable polymeric  $\mu$ C arrays can be fabricated on the basis of standard thermal IM using precisely machined metal molds. It is the aim of the present scientific activities to adapt IM, well established on the millimeter scale and above, to molds with 30  $\mu$ m-thin cavities, 500  $\mu$ m long and 100  $\mu$ m wide to realize polymer  $\mu$ Cs with a performance comparable to the presently used silicon-based arrays (hence termed micro-injection molding ( $\mu$ IM)). Sensitivity enhancement using customized surface structuring within the mold cavity is also being studied.

## 2. Materials and methods

### 2.1. Comparing established rigid $\mu$ Cs with polymeric ones

$\mu$ Cs respond to impacts ranging from surface stress via mass change to temperature. Their sensing involves the detection of  $\mu$ C deflections and of  $\mu$ C resonance frequencies. The laser beam projection technique provides the  $\mu$ C deflection induced by the forces acting on the cantilever [4]. Forces in the pN-range are detectable, since the setup can uncover sub-nanometer deflections of the apex of the  $\mu$ C sensors. These forces comprise expansions or contractions acting on one side of the cantilever surface [16]. One applies static and dynamic modes for more or less sophisticated sensing. In static mode, the surface stress generated from selectively adsorbed molecules on one side of the cantilever is measured. The free-end deflection  $\Delta_z$  as the result of the surface stress  $\sigma_{surface}$  is often quantified using the well-known Stoney formula [4,7], for example in the form of Sader [17]:

$$\Delta_z = \frac{3(1-\nu)L^2}{Et^2} (\Delta\sigma_{surface}) \quad (1)$$

where  $\Delta\sigma_{surface}$  is the difference of surface stress between top and bottom sides of the cantilever,  $\nu$  is the Poisson's ratio and  $E$  is the Young's modulus of the cantilever material and  $L$  and  $t$  are the length and thickness of the cantilever, respectively.

In dynamic mode, the resonance frequency of the cantilever  $f_{res}$  is monitored during mass adsorption on the cantilever [18]. The related shifts in resonance frequency  $\Delta f_{res}$  are given for homoge-

neously distributed adsorbents by

$$\Delta f_{res} \approx -f_{res} \frac{\Delta m}{2m_0} \quad (2)$$

where  $\Delta m$  is the absorbed mass and  $m_0$  is the initial mass of the cantilever [18]. The frequency shifts per mass change on the typically applied cantilever of rectangular shape is

$$\frac{\Delta f_{res}}{\Delta m_0} = \frac{1}{4\pi n_1 L^3 w} \sqrt{\frac{E}{\rho^3}} \quad (3)$$

with  $\rho = m/Lwt$  as mass density and  $n_1 \sim 1$  as characteristic geometrical  $\mu$ C parameter [1].

The frequencies for the  $i$ th resonance mode,  $f_i$ , can be estimated using the  $\mu$ C geometry,  $L$  and  $t$ , and the materials density  $\rho$ , 2330 and 3180 kg m<sup>-3</sup> for Si and Si<sub>3</sub>N<sub>4</sub> as well as 1220, 900, and 1220 kg m<sup>-3</sup> for the polymers polyvinylidene fluoride (PVDF), polypropylene (PP), and polyoxymethylene copolymers (POM-C), respectively:

$$f_i = \frac{t}{2\pi} \left( \frac{\alpha_i}{L} \right)^2 \sqrt{\frac{E}{12\rho}} \quad \alpha_i: \quad \alpha_1 = 1.9; \quad \alpha_2 = 4.7; \quad \alpha_3 = 7.8; \quad \dots \quad (4)$$

$\alpha_i$  is a constant obtained by numerically solving the beam frequency equation [7]. The  $Q$ -factor characterizes the resonator's bandwidth  $B$  relative to its centre frequency and the  $\mu$ C damping  $\delta$  during ring-off:

$$Q = f \frac{\pi}{\delta} = \frac{f}{B} \quad (5)$$

The sensitivity of the sensor depends on the mechanical parameters Young's modulus  $E$ ,  $\sim 130$ – $188$  GPa for Si, 310 GPa for Si<sub>3</sub>N<sub>4</sub>, as well as 6.7, 1.9 and 6.7 GPa for PVDF, PP, and POM, respectively, and Poisson ratio  $\nu \sim 0.22$  for Si and 0.24 for Si<sub>3</sub>N<sub>4</sub> as well as 0.3–0.5 for most polymers. In order to fabricate polymer  $\mu$ Cs with sensitivity comparable with silicon ones (typical dimensions of  $L \sim 500$   $\mu$ m and 1–5  $\mu$ m thickness), while keeping  $L$  constant, the  $\mu$ Cs have to be one order of magnitude thicker to compensate the hundred times smaller  $E$ .

For the selective sensitivity to detect contaminants in gases or dedicated species in liquids, the cantilever surfaces have to be functionalized. For this purpose, one  $\mu$ C side is coated or patterned to enhance selective binding of the species of interest chemically or by featured surface morphology. Chung et al. [16], for example, used field ion beam milling to build nanostructures on the  $\mu$ C surfaces. The mechanical properties of the  $\mu$ Cs depend on the coating and its thickness as well as the morphological features including pattern sizes. Field ion beam milling modifications soften cantilevers [19,20], whereas corrugations generated by means of stencils stiffen cantilevers and membranes [21].  $\mu$ IM belongs to the attractive approaches to manufacture polymer  $\mu$ C with pre-defined surface microstructures.

### 2.2. Microinjection molding

A modular injection molding tool has been developed that consists of a high quality steel cylinder (Polmax Uddeholm) 30 mm in diameter as mold insert with two internal resistive heating cartridges (Watlow Firerod, 230 V, 180 W, 49 W/cm<sup>2</sup>) fixed in the three-plate molding tool 'handy mold' with ejector pins (see Fig. 1, left side). This setup enables us to proceed with both isothermal and variothermal heating schemes with short heating times for temperatures as high as 320 °C in the vicinity of the mold cavities. The tool is installed in the clamping unit of an Arburg 320 Allrounder (Arburg, Lossburg, Germany) with a maximum clamping force of 600 kN.

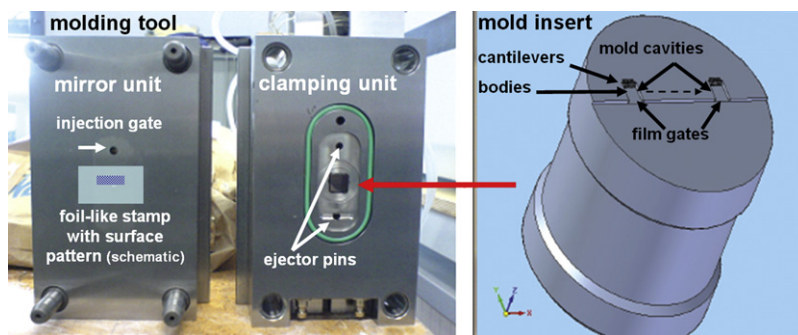


**Fig. 1.** Molding tool (handy mold) with two sides (left side). The mirror side contains the gate (top) and the location, where the patterned foil is placed. The clamping unit contains the mold insert (right side) with two mold cavities.

In contrast to the work of Andrew et al. [10] with one mold cavity composed of two halves placed in the opposite mold units of the IM machine to generate cantilevers with symmetric position, the present mold system comprises only one cavity located on the closing side [22,23]. The other side is free for mirror plates with designed micro- or nano-features.

The two parallel mold cavities (see Fig. 1, right side) were fabricated using laser ablation, and placed into the central part of the flat end of the cylinder. They are connected to the injection gate via a large plate-like cavity through 2.5 mm-wide gates for filling. The  $\mu$ C chip was designed with outlines of a micro-machined 500  $\mu$ m-thick silicon  $\mu$ C with a  $3.5 \times 2.5 \text{ mm}^2$  large body. It has eight 80–130  $\mu$ m-wide  $\mu$ C beams with a 500  $\mu$ m pitch on one side. The thickness chosen was usually in the range between 20 and 40  $\mu$ m. To guarantee fast and complete filling also molds with 60  $\mu$ m depths were applied (see Fig. 2, top micrograph). For the venting, at the end of each beam cavity thin, 5 mm-long,  $10 \times 10 \text{ }\mu\text{m}^2$ -wide channels were incorporated. The polished steel plate with one injection gate is the flat counterpart opposite to the closing unit. Therefore, the upper side of each  $\mu$ C beam has a polished finish (see Fig. 2, bottom micrograph) later used for laser beam reflection. Surface patterned beams require, thus, an additional mold insert with a micro- and nano-relief to be introduced at the mirror side. In place of another mold insert, we incorporate a thin, patterned polymer foil (see Fig. 1, left side). This foil-like mold prepared by hot embossing, typically 25–100  $\mu$ m thick, forms the interface between the two units

of the IM machine and is subjected to related pressure and heat. To ensure repeated alignment during injection and demolding, it is directly fixed onto the polished top by adhesive tape or clamps. The mold temperatures and pressures have to be low enough to enable a sufficient number of replications without degradation of the surface relief. The main advantage of the method lies in the simple integration of gratings with different sizes and orientations. It is particularly useful for test series. Even for mass production the method is promising, since polymer foils can be patterned in roll-to-roll processes [24,25].

### 2.3. Microinjection molded polymer materials

The polymers used are different grades of poly(etheretherketone) (PEEK: Solvay Advanced Polymer AvaSpire AV-650 BG15, Solvay Advanced Polymer KetaSpire KT-880NT, Victrex 150G), poly(propylene) (PP: Moplen SM 6100), polyoxymethylene copolymers (POM-C: 511P Delrin NC010), cyclic olefin copolymers (COC: Topas 8007X10), polyvinylidene fluoride (PVDF: Kynar 720 Arkema) and liquid crystal polymer (LCP: Vectra A 390).

### 2.4. Microinjection mold processes

Up to 160  $^{\circ}\text{C}$ , the tool temperatures were controlled by heated water. For the higher process temperatures up to 260  $^{\circ}\text{C}$  oil served as heat transport medium. The other process parameters are summarized in Table 1. As the foil mentioned above 100  $\mu$ m-thick polycarbonate (PC: Bayer Makrofol ID 6-2) and 25  $\mu$ m-thick PEEK (Aptiv 2000 series) were inserted. While PC with a glass transition temperature of 148  $^{\circ}\text{C}$  only allows molding polymers with rather low process temperatures, PEEK, which has a comparative glass transition temperature of 143  $^{\circ}\text{C}$  was considered as higher temperature alternative because of its excellent demolding properties. The PC and PEEK foils were hot embossed in a Jenoptik HEX 03 machine for a period of 10 min using temperatures of 160 and 175  $^{\circ}\text{C}$  and forces of 15 and 4 kN, respectively. As the molds for hot embossing, either surface patterned silicon wafers or replicas in Ormostamp both with anti-sticking layer were used [26,27].

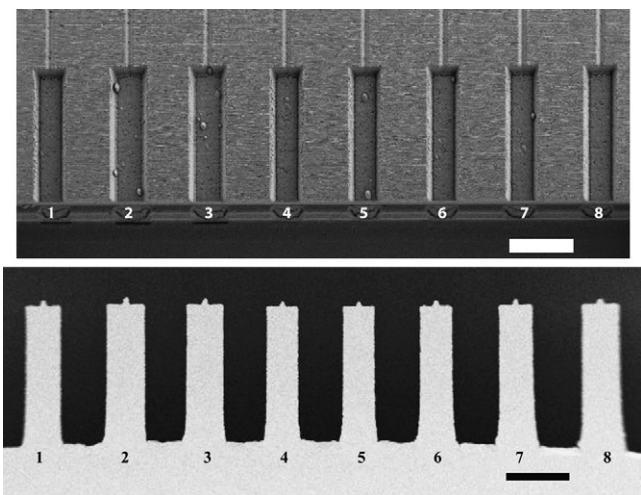


**Fig. 2.** The top SEM micrograph shows the array of eight laser ablated cantilever cavities in the steel mold insert. The cavity width varies from 80 to 130  $\mu$ m. The scale bar corresponds to 200  $\mu$ m. The SEM micrograph on the bottom is an image of an injection molded PP micro-cantilever array. Small tips at the cantilever end demonstrate the complete filling up to the venting channels.

**Table 1**  
Injection molding process parameters for the selected polymer materials including all grades of PEEK.

	COC	PP	PEEK	POM-C	LCP	PVDF
Melt temperature [ $^{\circ}\text{C}$ ]	240	200	400	220	300	220
Tool temperature [ $^{\circ}\text{C}$ ]	77	40	225	120	150	120
Mold insert temperature [ $^{\circ}\text{C}$ ]	77	40	260	120	150	120
Injection speed [ $\text{cm}^3/\text{s}$ ]	30	9	10	10	10	10

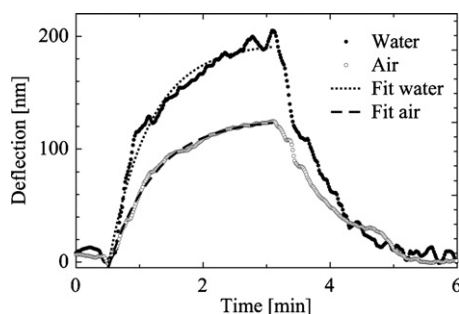


**Fig. 3.** Real time monitoring of injection molded PVDF  $\mu$ C deflection: heat test of 30  $\mu$ m-thick  $\mu$ Cs with a temperature increase from 25 to 35  $^{\circ}$ C at a heating rate of about  $t_{heat} = 0.5$  min and a temperature decrease back to 25  $^{\circ}$ C at a cooling rate of about  $t_{cool} = 3.2$  min.

### 2.5. Cantilever finishing

The injection molded  $\mu$ Cs were coated on the mirror side with 20 nm-thin gold films using a thermal evaporator (Balzers BAE250). This film guarantees sufficient laser beam reflectivity to use the Cantisens<sup>®</sup> research system (Concentris GmbH, Basel, Switzerland) for measuring the deflection and the resonance frequency of the  $\mu$ C. Replication quality was analyzed using scanning electron microscopy (SEM: Supra 55 VP, Carl Zeiss NTS GmbH, Oberkochen, Germany), after coating with a thin layer of PdAu.

## 3. Results

Complete filling of the mold cavities was observed for all polymers using isothermal  $\mu$ IM (Fig. 2, bottom micrograph for PP) with the exception of the high-performance polymer PEEK, which requires mold temperatures of up to 320  $^{\circ}$ C and processing temperatures higher than 260  $^{\circ}$ C. We have not observed any degradation for PP, COC, POM-C, and PVDF. However, with PEEK, which is more sensitive to longer residence time, visible signs of degradation were observed. Also with the patterned foil-like molds, using standard isothermal  $\mu$ IM process parameters, a complete filling of high-aspect-ratio micro-cavities was achieved for PP (see Fig. 5). The mold temperature was low enough to use the polymeric foils for several hundreds replications without degradation of the surface relief.

With the exception of PEEK, the cantilevers reveal the expected thermal behavior as demonstrated in the diagram in Fig. 3 for the gold-coated PVDF cantilever under atmospheric conditions, i.e. in air, and in liquid (water). The heat tests included a temperature cycle with an increase from 25 to 35  $^{\circ}$ C and a subsequent decrease back to 25  $^{\circ}$ C within a time of about 4 min. The heat tests prove the sensitivity of the cantilevers that corresponds to deflections of the order of 10 nm. The deflection signal exhibits an exponential, asymptotic behavior as confirmed by the fits in Fig. 3. For the temperature difference of 10 K the maximal deflection for PVDF  $\mu$ Cs in air corresponds to  $(95 \pm 16)$  nm and  $(55 \pm 5)$  nm for thicknesses of 30  $\mu$ m and 40  $\mu$ m, respectively. In water, these values should be similar but gave higher values, namely  $(127 \pm 17)$  nm and  $(154 \pm 55)$  nm. Note the larger scattering of the data in liquid, which indicates less stable experimental conditions and reduced reproducibility in liquid compared to air.

The Cantisens<sup>®</sup> Research system permits the experimental determination of resonance frequencies  $f_{res}$  and quality factors  $Q$  for the polymeric  $\mu$ Cs. Table 2 summarizes the mean values and related standard deviations of the resonance frequency measurements for the  $\mu$ Cs in air and water. The deviations of the experimental data from the estimated ones are reasonably explained accounting for dimensional variations as well as the frequency dependence on  $E$ .

**Table 2**

Mean values and related standard deviations of the resonance frequency  $f_{res}$  as well as quality factor  $Q$  in air and water.

$\mu$ C thickness and polymer	30 $\mu$ m PP	40 $\mu$ m PP	30 $\mu$ m PVDF	40 $\mu$ m PVDF	30 $\mu$ m POM-C
$f_{res}$ in air (experimental) [kHz]	$48 \pm 3$	$50 \pm 1$	$60 \pm 3$	$79 \pm 5$	$60 \pm 4$
$f_{res}$ (theoretical, Eq. (4))	38	46	66	88	78
$f_{res}$ in water (experimental) [kHz]	$37 \pm 8$	$33 \pm 27$	$43 \pm 5$	$52 \pm 5$	$36 \pm 7$
$Q$ -factor in air	28	46	38	19	33
$Q$ -factor in water	20	11	10	9	19

The drop in resonance frequency in water results from the damping, which lowers the  $Q$ -factor of the  $\mu$ Cs as given in Table 2. The  $Q$ -factors were estimated directly from the frequency spectra [1,2,4].

The stiffness of the  $\mu$ Cs was determined by nanoindentation of the injection molded PP  $\mu$ Cs. The measurements were carried out using a nanoindenter (MTS XP<sup>®</sup> with a Berkovich tip (XPT-12761-0)). The unloading segment of the measured load–displacement curve in nanoindentation permits an estimation of the cantilever's Young's modulus, by defining the elastic stiffness as the slope of the unloading segment [28]. The obtained value of 2.4 GPa is close to the value (1.9 GPa) mentioned in the technical datasheet from the PP supplier.

As a first attempt towards biosensing, the chemisorption of thiols on gold coated  $\mu$ Cs was recorded by means of the Cantisens<sup>®</sup> Research system. The data of six PVDF 60  $\mu$ m-thick  $\mu$ Cs from an injection molded array are shown in the diagram of Fig. 4. The deflection results from the surface stress, that is generated during the self-assembly of thiol molecules on the gold-coated substrate. Using the Stoney formula (1), the surface stress values can be determined to derive the sensitivity of the individual  $\mu$ C sensors. Although the curves in Fig. 4 exhibit the expected characteristic behavior, the maximal amplitudes differ by up to a factor of three.

3D corrugation patterns have been applied to enhance the stability of membranes and their stiffness against bending [21]. Therefore, 5  $\mu$ m-wide stripes as presented in Fig. 5 were introduced into the mold and tested for cantilevers, too. Preliminary experiments show that 5  $\mu$ m-deep trenches, when oriented parallel to the beam, enhance the resonance frequency, and also serve as a means to stiffen cantilevers against torsion (see Fig. 6). For separation of different patterns, only a rough alignment of the stripe patterns needs to be ensured. However, as can be seen in Fig. 6, due to the softening of the polymer mold during injection, the venting channels can be closed, leading to an incomplete filling of the mold cavities. This seems more likely with 1  $\mu$ m-deep stripes in Fig. 6, particularly if they are oriented perpendicularly and not parallel to the beam.

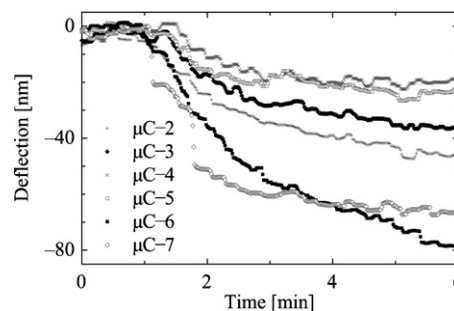


**Fig. 4.** Real-time monitoring of injection molded PVDF  $\mu$ C deflection in static mode. Formation of mercaptohexanol self-assembled monolayers on gold-coated 60  $\mu$ m-thick  $\mu$ Cs.

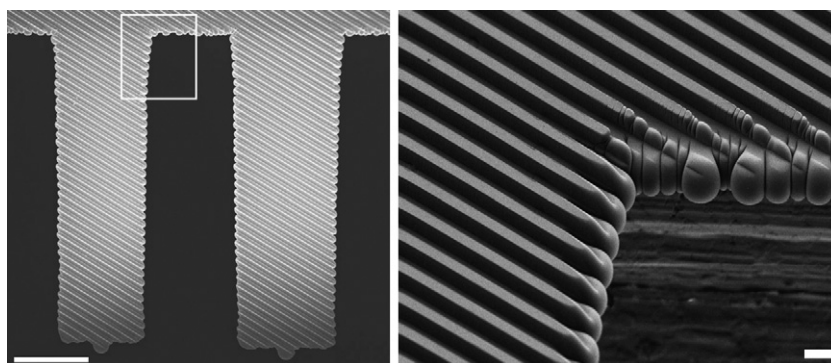


**Fig. 5.** SEM micrographs of the line pattern (period 10  $\mu\text{m}$ , depth 5  $\mu\text{m}$ , width 5  $\mu\text{m}$ ) transferred during the  $\mu\text{IM}$  process from a foil-like mold to the surface of two molded  $\mu\text{C}$  (left side). In contrast to the non-patterned original beams, the surface patterned beams are slightly (10%) wider due to high injection pressure and the softness of the PC foil (see extract at right side). The scale bar for the left micrograph corresponds to 100  $\mu\text{m}$  and right micrograph corresponds to 10  $\mu\text{m}$ .

#### 4. Discussion

The incorporation of a foil-like mold with well-defined microstructures into the molding tool is a relatively simple approach to build microstructures on the polymer cantilevers. One can easily change the design, the size and the orientation of the pattern as demonstrated by the micrographs in Figs. 5 and 6. The orientation of the lines along the  $\mu\text{Cs}$  is controlled without changing the device dimensions and outlines. Deep longitudinal stripes aligned within 5  $\mu\text{m}$  precision promote the complete filling of the mold cavities and, hence, give rise to fully molded cantilevers. Moreover, these longitudinal channels are preferred for the contractile cell force measurements [29] as cells generally orient themselves along the ridges. Deep trenches with directions perpendicular to the beams can lead to a slight broadening of the cantilever, since material can flow in the trenches of the softened foil-like mold during injection. Different orientations, depths and patterns will be tested in future.

The differences of the heat tests in water and air are associated with an artifact, which results from the optical refraction at the air–water interface in the Concentris system. This also explains the larger data scattering. However, the main reason for the large tolerances observed in the experimental data is due to the fact the current mold exhibits large dimensional variations and a large surface roughness. The latter may be responsible that during demolding, high demolding forces induce intrinsic stress and distortion. This will be improved by using molds with reduced surface roughness.

The thiol adsorption measurements elucidate the necessity of calibration before reproducible experiments can be performed. As noted before, the deflection variations between the cantilevers originate mainly from the discrepancies in the  $\mu\text{Cs}$  geometry. Con-

sequently, the processing has to be improved or, alternatively, the obtained  $\mu\text{Cs}$  have to be precisely calibrated in a more or less individual fashion.

#### 5. Conclusions and outlook

$\mu\text{IM}$  permits the fabrication of polymeric  $\mu\text{C}$  arrays with fair properties for biomedical applications. The choice of polymer material and geometry allows tailoring the sensor characteristics. The thiol-gold binding tests demonstrate that the prepared polymer  $\mu\text{Cs}$  are highly sensitive surface stress monitors. Recent studies have demonstrated the applicability of  $\mu\text{Cs}$  as olfactory sensors [30,31]. Last year one of the first clinical studies was published applying standard silicon  $\mu\text{Cs}$  for the detection of diseases [31]. In addition, polymer  $\mu\text{Cs}$  can be used to measure contractile cell forces [29]. By modifying its surface morphology or chemistry one can mimic implant surfaces and can compare the influence on the cell response. Thus, the microstructured  $\mu\text{C}$  array sensors will support the selection of advanced surface-modified substrates and medical implant surfaces.

Initial mechanical and functional tests imply that these polymer  $\mu\text{Cs}$  are mechanically compliant for use in biochemistry and biomedicine. An additional advantage is that the polymer cantilevers can be modified adding micro- and nano-patterns to the mold cavities [32–34]. It is expected that by choosing appropriate sizes and orientations of the surface microstructures, the mechanical properties of individual  $\mu\text{Cs}$  with identical outlines can be modified, e.g. by softening (line ridges perpendicular to beam) or stiffening (line ridges along beam) of the beam. Surface structuring can also tailor cell locomotion, adhesion and spreading, which are closely related to the contractile cell forces to be quantified. The

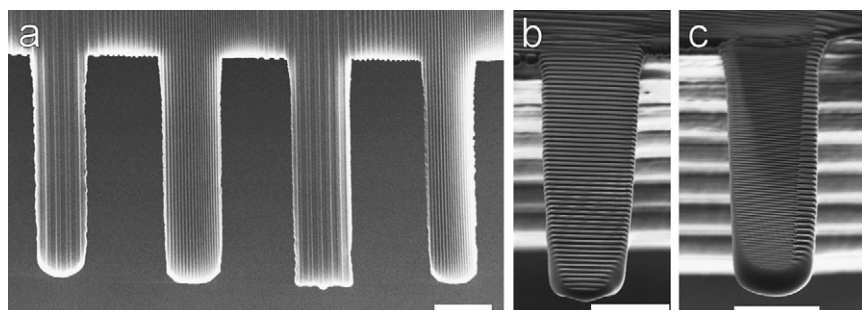


**Fig. 6.** SEM micrographs of PP  $\mu\text{Cs}$  line patterns (depth 1  $\mu\text{m}$ ) (a) with different periods in the direction of beams and (b), (c) perpendicular to beams (right side), (c) with two patterns on one beam. The scale bars corresponds to 100  $\mu\text{m}$ .

$\mu$ Cs patterning can be established for a range of cantilever designs. Once successfully established, the polymer-based  $\mu$ C systems will permit to gain major cost reductions and to address further applications in the field of biomedicine.

### Acknowledgement

This activity is funded by the Swiss Nanoscience Institute (SNI) through the applied research project DICANS, a collaborative initiative between the Biomaterials Science Center (BMC) of the University of Basel, Paul Scherrer Institut (PSI), University of Applied Sciences Northwestern Switzerland (FHNW) and Concentris GmbH. The authors would like to thank K. Jefimovs (EMPA Dübendorf) for the laser micro-machining of the mold, R. Ghisleni (EMPA Thun) for his assistance with the MTS XP<sup>®</sup> system, J. Köser (FHNW Muttentz) for his advice on using the Cantisens<sup>®</sup> research system and the members from the LMN-PSI, for their technical assistance. The Solvay PEEK grades used in this study was kindly supplied by Bigler AG. The MTS XP<sup>®</sup> system used in this study is maintained and operated by EMPA Thun.

### References

- [1] H.P. Lang, M. Hegner, Ch. Gerber, Nanomechanical cantilever array sensors, in: B. Bhushan (Ed.), Handbook of Nanotechnology, Springer Verlag, Berlin/Heidelberg, 2010, pp. 427–452.
- [2] B. Bhushan, O. Marti, Scanning probe microscopy – principle of operation, instrumentation, and probes, in: B. Bhushan (Ed.), Handbook of Nanotechnology, Springer Verlag, Berlin/Heidelberg, 2010, pp. 573–617.
- [3] D. Lange, O. Brand, H. Baltes, CMOS cantilever sensor systems, atomic-force microscopy and gas sensing applications, in: Microtechnology and MEMS VIII, 2002, p. 150.
- [4] R. Berger, Ch. Gerber, H.P. Lang, J.K. Gimzewski, Micromechanics: a toolbox for femtoscale science: “towards a laboratory on a tip”, Microelectron. Eng. 35 (1997) 373–379.
- [5] H.P. Lang, R. Berger, F. Battiston, J.-P. Ramseyer, E. Meyer, C. Andreoli, J. Brugger, P. Vettiger, M. Despont, T. Mezzacasa, L. Scandella, H.-J. Güntherodt, Ch. Gerber, J.K. Gimzewski, A chemical sensor based on a micromechanical cantilever array for the identification of gases and vapors, Appl. Phys. A 66 (1998) S61–S64.
- [6] M. Toda, Y. Joseph, R. Berger, Swelling of Composite Films at Interfaces, J. Physical Chemistry C 114 (2010) 2012–2017.
- [7] K. Geoders, J. Colton, L. Bootomley, Microcantilevers: sensing chemical interactions via mechanical motion, Chem. Rev. 108 (2008) 522–542.
- [8] A. Vidic, D. Then, Ch. Ziegler, A new cantilever system for gas and liquid sensing, Ultramicroscopy 97 (2003) 407–416.
- [9] G. Genolet, M. Despont, P. Vettiger, D. Anselmetti, All-photoplastic, soft cantilever cassette probe for scanning force microscopy, J. Vac. Sci. Technol. B 18 (2) (2000) 617–620.
- [10] M.A.P. Andrew, W. McFarland, L.A. Bottomley, J.S. Colton, Injection moulding of high aspect ratio micron-scale thickness polymeric microcantilevers, Nanotechnology 15 (2004) 1628–1632.
- [11] M. Hecke, Review on micro molding of thermoplastic polymers, J. Micromech. Microeng. 14 (2004) R1–R14.
- [12] J. Giboz, T. Copponnex, P. Mélé, Microinjection molding of thermoplastic polymers: a review, J. Micromech. Microeng. 17 (2007) 96–109.
- [13] H. Schiff, S. Bellini, J. Gobrecht, Perforated polymer membranes fabricated by nanoimprint lithography, Microelectron. Eng. 83 (2006) 873–875.
- [14] H. Schiff, S. Bellini, U. Pieleas, J. Gobrecht, Sustained polymer membranes fabricated by nanoimprint lithography, J. Microlith. Microfab. Microsyst. 5 (2006) 011010.
- [15] H. Schiff, C. David, M. Gabriel, J. Gobrecht, L. Hyderman, W. Kaiser, S. Körpel, L. Scandella, Nanoreplication in polymers using hot embossing and injection molding, Microelectron. Eng. 53 (2000) 171–174.
- [16] E. Chung, N. Lavrik, P. Datskos, J. McFarlane, S. Dai, C. Tsouris, Microcantilever sensors with chemically selective coatings of ionic liquids, AIChE J. 53 (10) (2007) 2726–2731.
- [17] M. Calleja, J. Tamayo, L.M. Lechuga, A. Boisen, Highly sensitive polymer-based cantilever-sensors for DNA detection, Ultramicroscopy 105 (2005) 215–222.
- [18] S.K.M. Nordström, M. Lillemose, A. Johansson, S. Dohn, D. Haefliger, G. Blagoi, M. Havsteen-Jakobsen, A. Boisen, SU-8 cantilevers for bio/chemical sensing; fabrication, characterisation and development of novel read-out methods, Sensors 8 (2008) 1595–1612.
- [19] J.-H. Fabian, L. Scandella, H. Fuhrmann, R. Berger, T. Mezzacasa, Ch. Musil, J. Gobrecht, E. Meyer, Finite element calculations and fabrication of cantilever sensors for nanoscale detection, Ultramicroscopy 82 (2000) 69–77.
- [20] J.-H. Fabian, L. Scandella, T. Mezzacasa, D. Bächle, J. Gobrecht, P. Lerch, E. Meyer, Fabrication of micromechanical cantilever sensors for nanoscale thermal detection, Ultramicroscopy 83 (2000) 873–875.
- [21] M.A.F. van den Boogaart, M. Lishchynska, L.M. Doeswijk, J.C. Greer, J. Brugger, Corrugated membranes for improved pattern definition with micro/nanostencil lithography, Sens. Actuators A: Phys. 130–131 (2006) 568–574.
- [22] P. Urwyler, O. Häfeli, H. Schiff, J. Gobrecht, B. Müller, Disposable polymeric micro-cantilever arrays for biomedical applications, Eur. Cells Mater. 20 (2010) 48.
- [23] P. Urwyler, O. Häfeli, H. Schiff, J. Gobrecht, F. Battiston, B. Müller, Disposable polymeric micro-cantilever arrays for sensing, in: Proc. Eurosensors XXIV, September 5–8, Linz, Austria, 2010.
- [24] H. Schiff, Roll embossing and roller imprint, in: Y. Hirai (Ed.), Science and New Technology in Nanoimprint, Frontier Publishing Co Ltd, Japan, 2006, pp. 74–89.
- [25] T. Mäkelä, T. Haatainen, P. Majander, J. Ahopelto, V. Lambertini, Continuous double-sided roll-to-roll imprinting of polymer film, Jpn. J. Appl. Phys. 47 (6) (2008) 5142–5144.
- [26] H. Schiff, Nanoimprint lithography: an old story in modern times? A review, J. Vac. Sci. Technol. B 26 (2) (2008) 458–480.
- [27] H. Schiff, C. Spreu, M. Saidani, M. Bednarzik, J. Gobrecht, A. Klukowska, F. Reuther, G. Gruetzner, H.H. Solak, Transparent hybrid polymer stamp copies with sub-50 nm resolution for thermal and UV-nanoimprint lithography, J. Vac. Sci. Technol. B 27 (6) (2009) 2846–2849.
- [28] S.R. Kalidindi, S. Pathak, Determination of the effective zero-point and the extraction of spherical nanoindentation stress-strain curves, Acta Mater. 56 (2008) 3533–3542.
- [29] J. Köser, J. Gobrecht, U. Pieleas, B. Müller, Detection of the forces and modulation of cell-substrate interactions, Eur. Cells Mater. 16 (2008) 38.
- [30] F. Battiston, J. Ramseyer, H.P. Lang, M. Baller, Ch. Gerber, J. Gimzewski, E. Meyer, J. Güntherodt, A chemical sensor based on a microfabricated cantilever array with simultaneous resonance-frequency and bending readout, Sens. Actuators B 77 (2001) 122.
- [31] D. Schmid, H. Lang, S. Marsch, Ch. Gerber, P. Hunziker, Diagnosing disease by nanomechanical olfactory sensors, Eur. J. Nanomed. 1 (2008) 44.
- [32] V. Seena, N.S. Kale, S. Mukherji, V. Ramgopal Rao, Development of polymeric microcantilevers with novel transduction schemes for biosensing applications, Solid State Sci. 11 (9) (2009) 1606–1611.
- [33] J. Plaza, Villanueva, C. Dominguez, Novel cantilever design with high control of the mechanical performance, Microelectron. Eng. 84 (5–8) (2007) 1292–1295.
- [34] X.R. Zhang, X. Xua, Development of a biosensor based on laser-fabricated polymer microcantilevers, Appl. Phys. Lett. 85 (12) (2004) 2423–2425.

### Biographies

**Prabitha Urwyler** received her Bachelor of Technology (B.Tech.) in Computer Engineering from the Mangalore University, India in 1995. She worked as a software engineer at Melstar Information Technologies Ltd, India from 1995 to 1997 and later at the Swiss News Agency (SDA-ATS), Switzerland until 2008. She pursued her masters in 2006, which earned her M.Sc. in Biomedical Engineering from the University of Bern in 2008. She is currently working towards her PhD degree in Biomedical Engineering on the fabrication, characterization and application of disposable micro-cantilevers for biomedical applications at the University of Basel and the Paul Scherrer Institut.

**Helmut Schiff** received his diploma in Electrical Engineering from the University of Karlsruhe, Germany. He performed his Ph.D. studies at the Institute of Microtechnology Mainz (IMM), Germany. After his graduation in 1994, he joined PSI as a research staff member and is now head of the INKA-PSI Group in the Laboratory for Micro- and Nanotechnology at the PSI. He is actively involved in the development of nanoimprint lithography (NIL) as an alternative nanopatterning method for device fabrication. He is currently working in various national and international projects on stamp fabrication, hybrid technologies and innovative 3-D nanomolding.

**Jens Gobrecht** studied physics at the Technical University of Berlin, and received his diploma in engineering in 1976, followed by his Ph.D. from the Fritz-Haber Institut of the Max-Planck Society in Berlin. In 1980/1981 he worked on a post-doc position at the National Renewable Energy Laboratory in Golden, USA. After that he worked for 12 years in various functions at the ABB Corporate Research Center in Baden, Switzerland. In 1993 he joined the PSI and created the Laboratory for Micro- and Nanotechnology. In 2005 he was appointed Professor at the University of Applied Sciences of Northwestern Switzerland (FHNW) and head of the Institute of Polymer Nanotechnology (INKA), a joint venture with PSI. In 2007 J. Gobrecht co-founded “Eulitha AG”, a company active in EUV-based nanolithography.

**Oskar Häfeli** received his diploma in tool design and construction in 1972. Since 1977, he is the chief of the Injection Molding laboratory at the Institute for Polymer Engineering (IKT) at FHNW. He is actively involved in disseminating education, supervising various bachelor, master and Ph.D. Theses. His current work also includes research and development in the field of composites, natural fibers, micro- and nanoreplication for medical technology.

**Mirco Altana** received his diploma in Mechanical Engineering from the University of Applied Sciences Northwestern Switzerland in 2006. Currently he is pursuing his masters in Micro- and Nanotechnology at the University of Applied Sciences Vorarlberg in Dornbirn, Austria. He is working as a scientific assistant at the Institute of Polymer Nanotechnology (INKA) specializing in surface functionalization using nanoimprint lithography (NIL) and polymer functionalization.

**Felice Battiston** holds a degree in Electrical and Electronics Engineering and got a Ph.D. in Physics from the University of Basel in 1999. He worked as a post-doc at the University of Basel. Currently, he is the CTO of Concentris GmbH, which he founded in 2000.

**Bert Müller** received a diploma in mechanical engineering (1982), followed by the M.Sc. degree from the Dresden University of Technology and the Ph.D. from the University of Hannover, Germany in 1989 and 1994. From 1994 to 2001,

he worked as a researcher at the Paderborn University, Germany, EPF Lausanne, ETH Zurich. He became a faculty member of the Physics Department at ETH Zurich in April 2001. After his election as Thomas Straumann-Chair for Materials Science in Medicine at the University of Basel, Switzerland and his appointment at the Surgery Department of the University Hospital Basel in September 2006, he founded the Biomaterials Science Center. He also teaches physics and materials science at the ETH Zurich and the Universities of Basel and Bern.